Thermodynamic and structural aspects of the aqueous uranium(IV) system – hydrolysis vs. sulfate complexation

Lehmann, S.; Foerstendorf, H.; Zimmermann, T.; Patzschke, M.; Bok, F.; Brendler, V.; Stumpf, T.; Steudtner, R.;

Originally published:

November 2019

Dalton Transactions 48(2019), 17898-17907

DOI: https://doi.org/10.1039/C9DT02886B

Journal Name

ARTICLE

Thermodynamic and structural aspects of the aqueous uranium(IV) system – hydrolysis vs. sulfate complexation

Received 00th January 20xx,
Accepted 00th January 20xx

DOI: 10.1039/x0xx00000x

www.rsc.org/

Susanne Lehmann,[a] Harald Foerstendorf,[a] Thomas Zimmermann,[a,b] Michael Patzschke,[a] Frank Bok,[a] Vinzenz Brendler,[a] Thorsten Stumpf [a] and Robin Steudtner *[a]

The aquatic species of U(IV) in acidic aqueous solution in the presence of sulfate was studied in the micromolar range by a combined approach of optical spectroscopies (UV/vis and mid-IR), quantum-chemical calculations (QCC), and thermodynamic modelling. The number of species occurring in solution within the pH range 0–2 was assessed by decomposition and fitting of photometric spectra using HypSpec and Geochemist's Workbench software. Single component spectra of U^{4+}, UOH^{3+}, USO_4^{2+} and $U(SO_4)_2$ were obtained and extinction coefficients ε_λ have been calculated to be 58.8, 19.2, 47.6 and 40.3 L mol^{-1} cm^{-1}, respectively. Complex formation constants of two U(IV) sulfate species and the first hydrolysis species UOH^{3+} in infinite diluted solution were determined by thermodynamic modelling to be $\log \beta^{\Theta}_{101} = 6.9 \pm 0.3$, $\log \beta^{\Theta}_{102} = 11.8 \pm 0.5$ and $\log \beta^{\Theta}_{110} = -(0.36 \pm 0.1)$, respectively. No further U(IV) sulfate and hydrolysis species were observed under the prevailing conditions. Molecular structural information of the sulfate species was derived from vibrational spectra and QCC exhibiting a predominant monodentate coordination of the sulfate ions.

Introduction

To date thermodynamic data bases related to tetravalent uranium (U(IV)) essential for predicting speciation in aqueous solution is still sparse exhibiting large gaps in the understanding of fundamental hydrological processes and in the parameterization of its physicochemical properties.[1, 4] This is particularly due to a lack of appropriate analytic methods, concerning both, the generation of quantitative thermodynamic parameters and the spectroscopic evaluation of species stoichiometry and molecular structure. A quality assured thermodynamic data base for both tetra- and hexavalent uranium is, however, a prerequisite for a reliable predictive modeling of speciation and solubility limits under reducing conditions. Such conditions are of paramount importance for safety assessment of a future repository as well as for the remediation of the various legacies of uranium mining and milling. Thus, it is important to predict the environmental behavior of uranium in diluted to highly saline aquifer systems based on reliable thermodynamics with a realistic species set.

One important ligand to consider is sulfate (SO_4^{2-}), both in diluted and in highly saline solutions. For instance, sulfate is encountered in technological steps for both the mining and enrichment of uranium. Acid leaching of uranium ores was employed at mining sites, e.g. in Germany (Königstein in Saxony)[6] and Czechia (Stráž pod Ralskem in North Bohemia).[7]

In 2011, 46 % of world uranium mined originated from *in situ* leach (ISL) operations,[7] mostly with sulfuric acid due to the solubility of U(VI) sulfate complexes.[10] Most uranium mining in the U.S.A., Kazakhstan and Uzbekistan (and a significant part of that undertaken in Australia, China, and Russia) is now processed by ISL methods.[7]

The most up-to-date thermodynamic database concerning uranium chemistry lists two U(IV) sulfate complexes: USO_4^{2+} and $U(SO_4)_2$.[1] The formation constants were derived from solvent extraction,[11, 12] whereas other results from potentiometric or NMR experiments were discarded during the review process. It should be noted here, that the originally published values of [12] had been revised in [13].

In addition to the NEA TDB,[1] thermodynamic data from the JESS database[14] were examined. This revealed a large spread for values of $\log \beta$ of USO_4^{2+} and $U(SO_4)_2$, covering several orders of magnitude, e.g. $\log \beta_{101} = 2.52–9.0$, $\log \beta_{102} = 8–11.7$.[5, 15-17] Note, the abbreviation syntax β_{npq} is used for the formation constants of the complexes, where n denotes the number of uranium atoms, p the number of hydroxyl units, and q the number of sulfate ligands of each complex.

The considerable deviation of the $\log \beta$ values is most probably due to a broad range of experimental conditions applied, which in most cases included high ionic strengths, and to inconsistent extrapolations to infinite dilutions. Thus, we reviewed parameters used for thermodynamic calculations in terms of the activity coefficients considered. Extending the data survey to other tetravalent metal cations, it became

[a] Helmholtz-Zentrum Dresden-Rossendorf, Institute of Resource Ecology, Bautzner Landstr. 400, 01328 Dresden, Germany. E-mail: r.steudtner@hzdr.de
[b] Dresden University of Applied Sciences, Fakultät Landbau / Umwelt / Chemie, Pillnitzer Platz 2, 01326 Dresden.

† Electronic Supplementary Information (ESI) available. See DOI: 10.1039/x0xx00000x

obvious that the distribution of log β values within the respective aqueous sulfate systems – and even the number of species postulated – is not consistent at all. Consequently, a survey of all published complex stability constants for tetravalent actinide sulfates, extending to those of other tetravalent metal cations, was performed. Table 1 and Figure 1 provide the values rated as reliable, including the corresponding ionic radii[18] to visualize respective correlations. The listed constants β_{10n} refer to the equation:

$$M^{4+} + n\ SO_4^{2-} \leftrightarrow M(SO_4)_n^{(4-2n)+}.$$

Spectroscopic data of aqueous U(IV) sulfate species is still scarce. Up to date, EXAFS experiments have been carried out suggesting a monodentate and bidentate coordination of the sulfate ligand to the U(IV) ion as a function of sulfate concentration.[19, 20] Additionally, the formation of complexes in aqueous solution showing 1:4 and 1:5 stoichiometries, i.e. $[U(SO_{4,bid})_2(SO_{4,mon})_2 \times nH_2O]^{-4}$ and $[U(SO_4)_5H_2O]^{-6}$, respectively, are suggested.[19] However, related thermodynamic data is not provided.

The major goal of this study is to provide reliable thermodynamic data of the sulfate complexation with U(IV) based on spectroscopically verified species under a wide range of environmental conditions such as ionic strength *I*, pH, and concentrations of U(IV) and SO_4^{2-} in the submillimolar and millimolar range reducing uncertainties linked to activity corrections for infinite dilution. Accordingly, the derivation and verification of complex formation constants of the most prominent species, i.e. UOH^{3+}, $U(SO_4)_2$ and USO_4^{2+}, is addressed by photometric experiments. Finally, structural information of the sulfate species is expected to be obtained from vibrational spectroscopic data and quantum-chemical approaches.

Table 1 Standard complex stability constants log β°_{01n} for tetravalent metal cation sulfates* as a function of their effective ionic radius r (taken for eightfold coordination from[18]).

	r / pm	log β_{011}	log β_{012}	log β_{013}	log β_{014}	Ref.
Th	105	6.17 ± 0.32	9.69 ± 0.27	10.75 ± 0.08	8.44 **	2
U	100	6.58 ± 0.19	10.51 ± 0.20			1
		9.0	11.7			5
Np	98	6.85 ± 0.15	11.05 ± 0.25			1
		9.0	11.7			5
Pu	96	6.89 ± 0.22	11.14 ± 0.32			1
Zr	84	7.04 ± 0.09	11.54 ± 0.21	14.3 ± 0.50		9

*No values for Ce^{IV} or Hf^{IV} are published so far.

**The value is not a recommended one, but taken from Table IX-1 in [2]. There, no uncertainty estimate is given.

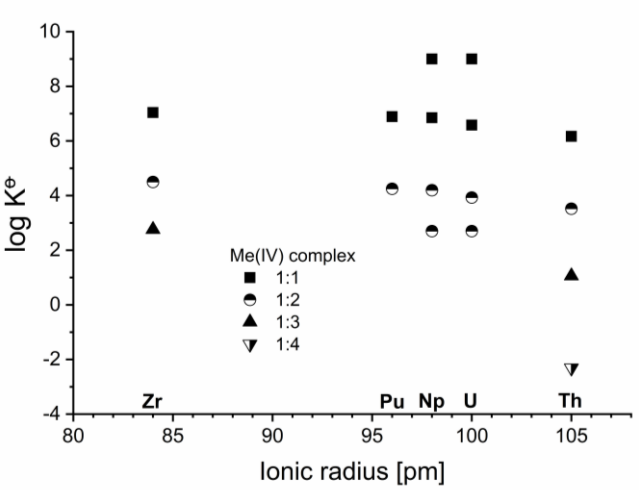

Figure 1: Stepwise complex formation constants for selected Me(IV) sulfates.

Experimental

Materials

Caution! Uranium (U) is a radioactive and chemically toxic element. Special precautions with suitable equipment and facility for radiation protection are required for handling its substances.

All solutions were prepared using reagent-grade chemicals and deionized, decarbonated water (Milli-Q). U(VI) stock solutions were prepared by dissolving $UO_3 \cdot 2.3\ H_2O$ (prepared from $UO_2(NO_3)_2 \cdot 6\ H_2O$, Chemapol, described in[21]) in 1 M $HClO_4$ (Merck p.A.) or HCl (Roth). The uranium concentration was confirmed by ICP-MS to be 10^{-2} mol·L^{-1}. All further sample preparation steps were carried out in an inert gas glove box with a purified nitrogen atmosphere (O_2 < 10 ppm) to avoid re-oxidation of U(IV) as well as carbonate complexation.

Electrochemical reduction

The U(VI) stock solutions were deoxygenated for at least 1 h with N_2 gas before electrochemical reduction. U(VI) was reduced to U(IV) in the cathodic part of an electrochemical H-cell whose anodic compartment was filled with an equimolar solution of $HClO_4$ or HCl, respectively. A Vycor glass diaphragm was employed to separate cathodic and anodic parts. Bulk electrolysis was performed for 4 h at a constant potential of −650 mV using an Autolab PGSTAT302 potentiostat (Eco Chemie B.V.) and a three electrode system: Pt working and counter electrode in the cathodic part and an Ag/AgCl (3 M NaCl) reference electrode in the anodic part (C3 Prozess- und Analysentechnik GmbH). The reduction was monitored by UV/vis spectra collected with Tidas 100 spectrophotometer (J&M Analytik AG). The residual content of U(VI) was determined by time-resolved laser-induced fluorescence spectroscopy (TRLFS, Inlite laser system, Continuum,

λ_{exc} = 266 nm, T = 25°C, E = 1 mJ, slit width 200 mm)[22] to be lower than 1%.

Analytical techniques

Uranium concentrations were confirmed using a Perkin Elmer ELAN 9000 inductively coupled plasma mass spectrometer (ICP-MS). PH values were determined using a microprocessor pH-Meter pMX 3000 coupled with Multiplex 3000 (WTW) and a 3 M KCl SenTix MIC electrode (WTW) calibrated against WTW buffer solutions (1.679, 4.006). The redox potential was measured using an InLab® Redox Micro electrode (VWR) and a pH 3110 (WTW).

Speciation calculations

Several series of thermodynamic speciation calculations were part of the work. They helped to define reasonable samples series compositions (see below) and were compared to results of the experimental series.

These calculations were carried out with the geochemical speciation code PHREEQC[23] whereas Pourbaix diagrams, i.e. pH–Eh predominance area diagrams for the U–S–O–H system at 25°C were computed with "Geochemist´s Workbench" Version 12.0.4 (Modul Phase2).[24] Both codes used thermodynamics data (complex formation constants and solubility products) from the most recent NEA TDB by Guillaumont et al.[1]

As the experimental set-up (as well as a variety of application areas aimed on) covers an ionic strength extending above 0.5 M (see Table 2), the commonly used extended Debye-Hückel approaches (namely the Davies equation[25]) to account for the ion-ion-interactions are not valid any longer. The switch to either the Specific Ion-interaction Theory (SIT)[26] or the Pitzer model[27] then requires a set of respective model parameters. SIT parameters can be taken from the most recent NEA TDB[28] amended by the parameters (and estimation functions) from the most recent release of the Nagra/PSI TDB[29]. An up-to-date set of respective Pitzer parameters for Uranium species is published in the 9th data release U(IV/VI) - Na, Mg, Ca, K - Cl, SO_4, $CO_3/HCO_3/CO_2$(g), Si - H_2O(l) (25°C) of the THEREDA TDB (www.thereda.de).[30] Tables SI 1 (SIT) and SI 2 (Pitzer) from the Supplementary Material† list all relevant values for the $U^{4+}/UO_2^{2+}/H^+/Cl^-/ClO_4^-/SO_4^{2-}$ system.

The redox potential of all sample solutions under the applied experimental conditions is approximately 0 mV. In this reducing environment uranium is expected to stay in the reduced oxidation state U(IV) as shown by the predominance area diagram shown in Figure 2.

For most of the important inorganic ligands the formation constants for U(IV) aqueous complexes are 1 - 4 orders of magnitude higher than for the respective U(VI) species, *cf.* table SI 3 in the Supplementary Material†. Thus it is expected that sulfate will stabilize the reduced form of uranium.

Selection of sample composition

Scoping chemical equilibrium diagrams were calculated at different pH, ionic strength, [U(IV)] and [SO_4^{2-}] at room temperature to identify species expected in representative aqueous solutions. This helped to define reasonable experimental conditions in order to gain appropriate spectra. These calculations were based on the speciation code PHREEQC in combination with the most recent release of the Nagra/PSI TDB[29] which is for uranium consistent with the NEA TDB by Guillaumont et al.[1]

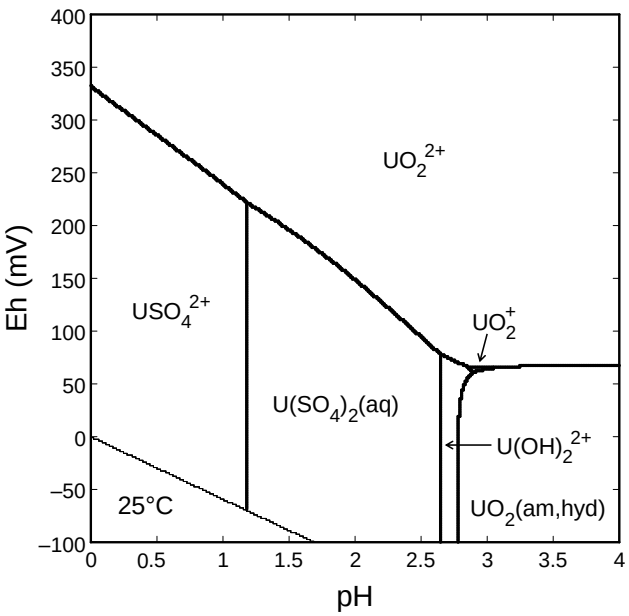

Figure 2: Predominance area diagram at 25°C calculated with Geochemist's Workbench under experimental conditions [U] = 60 µM and *I* = 0.15 M using data of NEA TDB[1].

Sample preparation

Table 2 shows the parameters of the solution series used for speciation determination. For each of the four sample series two stock solutions were prepared and mixed in different U(IV)/SO_4^{2-} ratios according to the methods of Yoe-Jones[31] and Job[32]. Sulfate was added to stock solutions by dissolving Na_2SO_4 (Fluka z.A.). Stock solutions were buffered to the same ionic strength using $NaClO_4 \times H_2O$ (Merck z.A.). The pH was adjusted by adding $HClO_4$ (Merck p.A.) and confirmed to be at the targeted value ± 0.05. At *I* = 1.2 M the pH discrepancy due to high ionic strength was considered following instructions of [33] with an $A_{c\ I=1.2}$ of 0.27.

Series 1 was prepared to investigate absorption properties of the free U^{4+} aquo ion at pH 0 and an ionic strength of 1 M. Therefore, U(IV) concentration was decreased from 100 µmol·L^{-1} to 0 µmol·L^{-1} in steps of 5 µmol L^{-1} by combining a uranium containing 1.0 M $HClO_4$ solution with pure 1.0 M $HClO_4$ solution in adequate proportions.

Series 2 was used to study U(IV) hydrolyses. Thus, U(IV) concentration was fixed to 100 µmol·L^{-1} and the pH was increased stepwise between 1.0 and 2.0. The ionic strength was buffered to 0.15 M. Series 3 and 4 were designed to prove U(IV) sulfate complexation with increasing sulfate concentration at two different ionic strengths.

Table 2: Sample series overview showing ranges of total $[U^{4+}]$ and $[SO_4^{2-}]$ as well as pH and *I* for particular sample series. $NaClO_4$ was used as background electrolyte.

series number	$[U^{4+}]$ / µmol L^{-1}	$[SO_4^{2-}]$ / µmol L^{-1}	pH	*I* / mol L^{-1}
1	0–100	0	0	1.0
2	100	0	1.0–2.0	0.15
3	60/63/65	0–5 000	1.0/1.5/2.0	0.15
4	100	0–10 000	0.0/1.0/2.0	1.2

Series 3 was buffered to an ionic strength of 0.15 M and measured at pH 1, 1.5 and 2 with U(IV) concentrations of 60, 63 and 65 µmol·L^{-1}, respectively, being comparable to uranium concentrations occurring in natural and anthropogenic environments. The sulfate concentration increases between 0 and 5 mmol·L^{-1}. Series 4 contains 100 µmol L^{-1} U(IV) and was buffered to an ionic strength of 1.2 M. The sulfate concentration increases stepwise from 0 to 10 mmol·L^{-1}. For pH 0.0 and 1.0 the maximum concentration of sulfate was 1.9 mmol·L^{-1}.

UV/vis measurements

To study the absorption properties of U(IV) in aqueous solution UV/vis absorption spectra were collected at room temperature (25°C) by a Tidas 100 spectrophotometer (J&M Analytik AG) coupled with a liquid waveguide capillary cell (LWCC) of 100 cm length (World Precision Instruments). Measurements were carried out under inert gas atmosphere in the same glove box where sample preparation took place.
All samples used for absorption spectroscopy were prepared directly before the spectroscopic measurements and measured by dynamic light scattering (Zetasizer Nano ZS, Malvern Instruments) to exclude precipitations. Uranium free solutions of equivalent composition were used as blanks for background subtraction.

UV/vis spectra analysis and derivation of complex formation constants using HypSpec

The program HypSpec[34, 35] was applied for derivation of complex formation constants, extinction coefficients and single component spectra of each species from multi component spectra gained by UV/vis. HypSpec can process UV/vis data, subject to the single requirement that the spectral intensity of each chemical species should be proportional to the concentration of that species in solution. The input data has to be adjusted to a certain ionic strength before using the program. Input parameters were the ICP-MS corrected uranium concentration, sulfate concentration, the pH of each sample and the optical path length used for UV/vis measurements.
The complex formation reaction of U^{4+} hydrolysis to be used by HypSpec is written as:

$$U^{4+} + H_2O(l) \leftrightarrow UOH^{3+} + H^+.$$

The deprotonation reactions of H_2SO_4 are then as follows:

$$HSO_4^- \leftrightarrow H^+ + SO_4^{2-}$$

$$H_2SO_4 \leftrightarrow 2\,H^+ + SO_4^{2-}.$$

The complex formation reaction of U^{4+} with sulfate can be written in general as:

$$U^{4+} + SO_4^{2-} \leftrightarrow USO_4^{2+}$$
$$U^{4+} + 2\,SO_4^{2-} \leftrightarrow U(SO_4)_2.$$

ATR FT-IR measurements

IR spectra were measured on a Bruker Vertex 70/v vacuum Fourier spectrometer equipped with an ATR accessory (DURA SamplIR II, Smiths Inc.), a horizontal diamond crystal (A=12.57 mm^2) with nine internal reflections on the upper surface and a Mercury Cadmium Telluride (MCT) detector (cut off: 580 cm^{-1}). Each single beam spectrum was averaged over 256 scans with a spectral resolution of 4 cm^{-1}. For suppression of background fluctuations, the measurements of the liquid samples were accomplished by using a flow cell that allows the subsequent acquisition of the spectra of the sample and reference solutions containing the sulfate (in absence or presence of U^{4+}) and the blank electrolyte, respectively.[36]

DFT calculations and electron density analysis

To support the IR measurements and gain further insight into the structure of U(IV) sulfate complexes a series of xTB (extended tight binding) and density functional theory (DFT) calculations was performed. The tight binding calculations were performed using the xTB program.[37] The very fast xTB results were used as starting structures for the DFT calculations. Vibrational spectra for the pre-optimized clusters were calculated to ensure that a true local minimum on the potential hyper-surface was found. All DFT calculations were done with the Turbomole[38] code version 7.1. The BP86 functional[39] was used in conjunction with an SV(P) basis set[40] and a relativistic small core effective core potential (ECP) for uranium.[41] Dispersion effects were taken into account by the method of Grimme[42] and solvation effects were included via the COSMO model[43] with an appropriate dielectric constant for water. The vibrational frequencies were computed numerically and solvent effects were taken into account. Because of the large size of the uranium-sulfate water clusters the vibrational frequencies were computed for the sulfate moiety alone. No inharmonic corrections were considered. The structure resembling the measured IR spectrum most closely was then subjected to a quantum theory of atoms in molecules (QTAIM) analysis using the AIMALL code.[44] Delocalization indices (DI) were extracted to see the influence on U(IV) complexation on the sulfate ion. The DI is a measure of the number of electrons shared between two atoms (two atomic basins) and it is related to the bond order.[45]

Results and discussion

Photometric studies of free U^{4+} aquo ion and of hydrolysis species UOH^{3+}

In a first step, single component spectra and extinction coefficients of the free U^{4+} aquo ion at pH 0 and of UOH^{3+} at pH 0-2 as well as the complex formation constant of the latter

species were directly derived from experiments based on sample series 1 and 2. In the first sample series, the absorption intensity decreased with decreasing U(IV) concentration, however, no modifications of the spectra's shapes were observed (Figure 3 A). The corresponding second derivatives revealed seven maxima at λ = 245.0, 430.2, 484.0, 495.8, 549.7, 649.8 and 671.9 nm (Table 3), which is in very good agreement with literature data.[46] The linear correlation between the absorption E_λ and the extinction coefficient ε_λ is described by the law of Lambert-Beer.

By linear approximation, an extinction coefficient of 58.8 ± 0.9 $L \cdot mol^{-1} \cdot cm^{-1}$ at 648.7 nm was derived for the free U^{4+} aquo ion. Kraus et al.[3] calculated 59 $L \cdot mol^{-1} \cdot cm^{-1}$ at an ionic strength of 1 M in chloric media.

With increasing pH in the samples of series 2, a significant change throughout the spectra occurred (Figure 3 B). At lower pH values, the absorption bands were identical to those of U(IV) aquo ion, whereas the intensities of the bands decreased and new absorption bands showed up with increasing pH.

In addition to the U(IV) absorption peak at 245 nm, a second peak at 265 nm occurred suggesting the formation of a new U(IV) species. Due to the high charge of the U(IV) ion, the hydrolysis occurred already at low pH values down to 0.5.[1] Therefore, this new species was attributed to the first hydrolysis species UOH^{3+}. There was no spectral evidence of further U(IV) hydrolysis species both in solution and as precipitations or colloid formations. We excluded U(IV) colloid formation in our samples as no change of the spectral background was observed. In particular, at shorter wavelengths a significant increase of the background absorption was generally observed upon formation of colloidal phases. This was explicitly demonstrated by experiments with solutions containing 1 mM U(IV) performed at increasing pH values up to 2.3 (Figure SI 2†). The findings are in agreement with recent results where U(IV) nanoparticle formation was observed at pH higher than 2 and elevated temperatures.[47]

The single component spectrum and extinction coefficient of U^{4+} gained for series 2 using HypSpec are in very good agreement with the results provided by series 1 with a slightly higher extinction coefficient of $\varepsilon_{648\,nm}$ = 63.3 L mol^{-1} cm^{-1}. The single component spectra of U^{4+} and UOH^{3+} are shown in Figure 3D. Peak maxima of UOH^{3+} absorption spectrum have been calculated by second derivative to be at λ = 265.0, 440.9, 469.5, 497.1, 526.0, 622.5 nm. The obtained complex formation constant was $\log \beta^{\circ}_{110,\, I = 0.15} = -(1.41 \pm 0.1)$. This constant is valid for an ionic strength of 0.15. In order to extrapolate to infinite dilution at T = 298 K, we used the Davies equation.[48] This led to a complex formation constant of $\log \beta^{\circ}_{110} = -(0.36 \pm 0.1)$ which is in good agreement with $\log \beta^{\circ}_{110} = -(0.34 \pm 0.20)$ reported by Fuger[8] and slightly higher than the proposed value by the NEA-TDB[1] of $\log \beta^{\circ}_{110} = -0.54 \pm 0.06$ (Table 3). The calculated extinction coefficient of UOH^{3+} is $\varepsilon_{622\,nm}$ = 19.2 L mol^{-1} cm^{-1} which is again in good agreement with literature data.[3] According to the lower extinction coefficient of UOH^{3+}, the total absorption intensity decreases with increasing UOH^{3+} concentration.

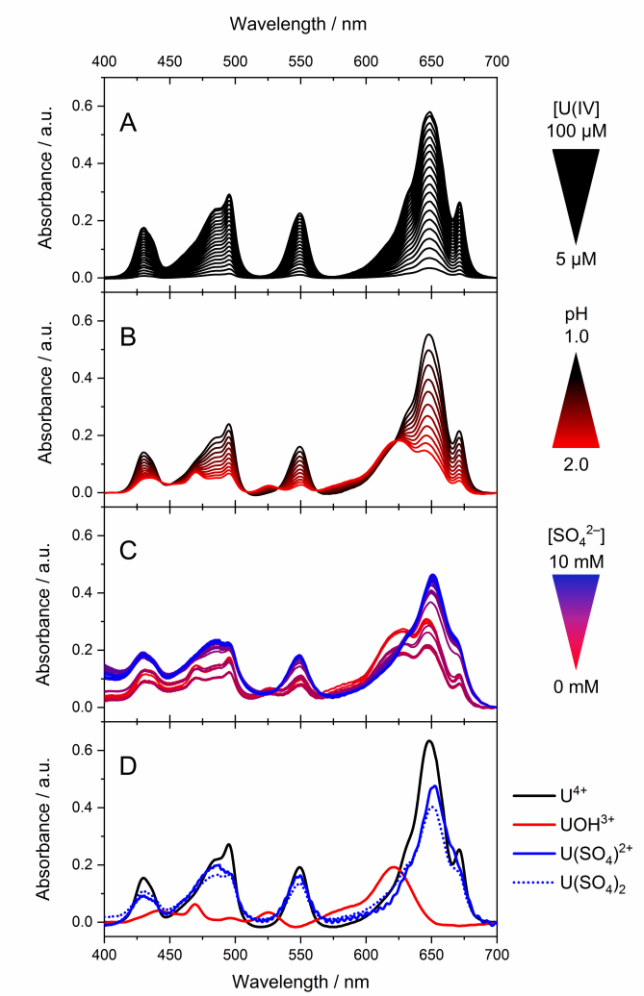

Figure 3: U(IV) UV/vis absorption spectra. A) As a function of uranium concentration at pH 0 and *I* = 1 M (series 1). B) as a function of pH at [U(IV)] = 100 µM and *I* = 0.15 M (series 2). C) Data set of series 4 at [U(IV)] = 100 µM, *I* = 1.2 M and pH 2 showing suppression of U(IV) hydrolysis by sulfate complexation with increasing sulfate concentration. D) Single component absorption spectra of U^{4+}, UOH^{3+}, $U(SO_4)^{2+}$ and $U(SO_4)_2$ at [U(IV)] = 100 µM with respective ε calculated using HypSpec.

These findings provide a basis for the study of the U(IV) sulfate system.

U(IV) sulfate complexation

Photometric studies. U(IV) sulfate complexation was studied within a sulfate concentration range from 0-10 mM, see Table 2 for detailed sample series compositions. Hence, the occurrence of multiple species such as free U^{4+}, first hydrolysis species UOH^{3+} and two U(IV) sulfate species had to be considered (Figure 2). At *I* = 0.15, pH 1 and low sulfate concentration, the absorption spectrum obtained was similar to the one of free U^{4+} at pH 0 showing a slightly lower absorption intensity due to hydrolysis (Figure SI 3†). With increasing sulfate concentration, a peak around 670 nm showed up interfering with the U^{4+} peak at 671.9 nm which obviously represents the formation of a sulfate species. At pH 1.5 and 2, the enhanced impact of hydrolysis and sulfate complexation became obvious by distinct spectral changes.

With increasing pH, the absorption intensity decreased already at low sulfate concentrations, which is due to hydrolysis. In contrast, the absorption intensity increased with increasing sulfate concentration due to formation of U(IV) sulfate complexes instead of UOH^{3+} (Figure 3 C, Figure 4).

At an ionic strength of 1.2 M, preliminary thermodynamic calculations suggested the formation of U(IV) sulfate species only at higher sulfate concentration than at I = 0.15 M. Thus, we considered an extended range of uranium and sulfate concentrations of 100 µM and 1.9 mM / 10 mM, respectively, at pH 0, 1 and 2. Contributions of free U^{4+}, UOH^{3+}, USO_4^{2+} and $U(SO_4)_2$ in solution were expected under these experimental conditions. Though, at pH 2 the $U(SO_4)_2$ fraction is predicted to be lower than at I = 0.15 M anyway (Figure SI 4[†]). At pH 0, the absorption spectra were in very good agreement to those of the fully hydrated U^{4+} implying the absence of sulfate complexation. At pH 1, we observed a decreased spectral intensity and increasing peak intensity at 670 nm which was attributed to proceeding sulfate complexation which became more obvious at pH 2. While in the absence of sulfate a reduced spectral intensity and characteristic absorption peaks of the fully hydrated U^{4+} ion and the hydrolysis species were observed, the formation of sulfate species became predominant instead characterized by an additional spectral feature at 670 nm and an increased spectral intensity with increasing sulfate concentration. The single component spectra of USO_4^{2+} and $U(SO_4)_2$ are shown in Figure 3 D in comparison to those of U^{4+} and UOH^{3+}. The spectra of both sulfate species show very similar properties. The most obvious differences are the higher peak shoulder of $U(SO_4)_2$ round about 670 nm and a slightly higher extinction coefficient of USO_4^{2+} $\varepsilon_{651\,nm} = 47.6\ L\ mol^{-1}\ cm^{-1}$ in comparison to $\varepsilon_{650\,nm} = 40.3\ L\ mol^{-1}\ cm^{-1}$ of $U(SO_4)_2$. Both values are between those of U^{4+} and UOH^{3+}. In comparison to the absorption spectra of the free U^{4+} aquo ion most significant modifications are between 450 and 500 nm as well as between 610 and 655 nm. No 1:3 complex or further complexes could be observed.

Complex formation constants derived from photometry. From the photometric data obtained, conditional complex formation constants log β_{npq} for USO_4^{2+} and $U(SO_4)_2$(aq) could be derived. Here, n denotes the number of uranium atoms, p the number of hydroxyl units, and q the number of sulfate ligands per complex. For USO_4^{2+}, two values, $\log \beta_{101,\ I = 0.15} = 5.02 \pm 0.1$ and $\log \beta_{101,\ I = 1.2} = 3.52 \pm 0.1$ were derived, yielding $\log \beta^{e}_{101} = 6.91 \pm 0.3$ and $\log \beta^{e}_{101} = 6.50 \pm 0.3$, respectively, when extrapolated to infinite dilution. These log β values for the 1:1 complex are close to the NEA recommendation of 6.58. For $U(SO_4)_2$(aq), we gained a complex formation constant of $\log \beta_{102,\ I = 0.15} = 9.00 \pm 0.1$ at I = 0.15. Extrapolation to infinite dilution led to $\log \beta^{e}_{102} = 11.84 \pm 0.5$, which is about one order of magnitude higher than that selected by NEA[1] but close to the value published by Rai et al. 1999[5] (Table 3). It has to be noted that the NEA recommendations are exclusively based on liquid-liquid extraction experiments performed at higher ionic strengths up to 2 M (mixtures of $NaClO_4$ & $HClO_4$) with tetradecylthioacetic acid (TTA) serving as the extracting organic phase and recalculations based on SIT[26]. Sulfate concentrations varied between zero and 0.1 or 0.0925 M, and temperatures were 10 and 25 °C in [11] and [12], respectively. The concentration of U(IV) was set to 0.0035 M in[12], whereas it varied between 0.0016 and 0.095 M in [11].

Rai et al. 1999[5] predicted similar values for different actinides at given ionic strength by reviewing numerous studies on log β values of tetravalent Th, U, Np and Pu sulfate which are taken into consideration by NEA as well. Therefore, they assumed that a reliable sulfate model for one of these actinides could be used to derive reasonable predictions also for similar systems of other actinides. Hence, they recommended Pitzer ion-ion-interaction parameters and log β values for the Np(IV) sulfate system as convenient analog for U(IV) until more reliable data becomes available. These values were gained by solvent extraction in dilute 0.1 M to concentrated 5 M NaCl and $NaClO_4$ at fixed pH[49] and solubility measurements of NpO_2 (am) in sulfate solutions as a function of pH. By

Table 3: Comparison of experimentally derived log β^{e} and ε values to literature for the complex formation reactions of U(IV) hydrolysis and U(IV) with sulfate in aqueous solution.

Reaction	Complex species	Stability constant log β^{e}		ε_λ / L mol^{-1} cm^{-1}		Main absorption bands / nm
		this work	literature	this work	literature	this work
	U4+			58.8 ± 0.9	59 [3]	245.0, 430.2, 484.0, 495.8, 549.7, 649.8, 671.9
$U^{4+} + H_2O \leftrightarrow UOH^{3+} + H^+$	UOH^{3+}	−0.36 ± 0.1	−0.54 ± 0.06 [1] −0.34 ± 0.2 [8]	19.2	20 [3]	265.0, 442.1 440.9 469.5 497.1 526.0 622.5
$U^{4+} + SO_4^{2-} \leftrightarrow USO_4^{2+}$	USO_4^{2+}	6.9 ± 0.3 from I = 0.15 M 6.5 ± 0.3 from I = 1.2M	6.58 ± 0.19 [1] 9.0 [5]	47.6		431.3 488.1 496.9 548.8 650.5 670.6
$U^{4+} + 2\ SO_4^{2-} \leftrightarrow U(SO_4)_2$	$U(SO_4)_2$	11.8 ± 0.5 from I = 1.2M	10.51 ± 0.20 [1] 11.7 [5]	40.3		430.7 483.9 496.5 549.4 650.3 671.3

comparison of speciation calculations using thermodynamic data gained with this study and data of NEA, it is obvious that the $U(SO_4)_2$ fraction is underestimated in NEA based calculations due to the lower log β value (Figure 4). Results have been used to determine reasonable sample composition for vibrational spectroscopy.

Structural aspects of USO_4^{2+}

The vibrational modes of small molecules observed in vibrational spectra intrinsically correlate with the overall molecule's symmetry. For the tetrahedral SO_4^{2-} anion, a triply degenerated asymmetric mode $\nu_3(SO_4)$ was observed at 1100 cm^{-1}.[50] The corresponding symmetric mode $\nu_1(SO_4)$ is generally inactive in IR spectra due to symmetry reasons, however, it might become weakly active and was observed around 980 cm^{-1} in aqueous solution.[50] The HSO_4^- anion exhibits a C_{3v} symmetry where the ν_3 mode splits into two modes ($\nu_{3,as}$ and $\nu_{3,s}$) due to a partial abrogation of the triply degenerated mode. Simultaneously, the ν_1 mode becomes IR active. Hence, the spectrum of the sulfate solution recorded at pH 1 (Figure 5A, dotted trace) represented a mixture of the anions SO_4^{2-} and HSO_4^-. The bands at 1191, 1051, and 884 cm^{-1} were assigned to the $\nu_{3,as}$, $\nu_{3,s}$, and the ν_1 modes of the monoanion, respectively, whereas the band at 1110 cm^{-1} represented the ν_3 mode of the SO_4^{2-} ion.

The spectrum of the U^{4+} containing solution revealed a significantly changed spectrum showing three band maxima at 1148, 1039 and 963 cm^{-1} (Figure 5 A, solid trace), which were ascribed to the $\nu_{3,as}$, $\nu_{3,s}$, and the ν_1 modes of the sulfate ions, respectively. From the pattern of bands suggesting a predominant C_{3v} symmetry of the sulfate ions, and from the strongly shifted frequencies, a monodentate coordination of the sulfate ions to the U^{4+} ion was derived. A bidentate coordination necessarily results in a C_{2v} symmetry, which in turn would imply a further splitting of the degenerated ν_3 mode into three bands, which was not observed in the spectra of this work. Additionally, a further verification of the assignment to a C_{3v} symmetry was achieved by spectral decomposition and fitting of the single components of the spectra shown in Fig. SI 6[+]. It could be shown that the spectra were excellently reproduced by the components necessary for C_{3v} symmetry of the sulfate ions coordinated to the U^{4+} ion (see Supporting Information).

DFT calculations

With the obtained IR results it is possible to compare computed IR spectra of suggested structures. Some important issues have to be considered before starting such calculations. The effects of the first solvation shell have to be taken into account explicitly. We have done so by starting with a USO_4 species and the adding water molecules to fill the coordination shell of uranium and the sulfate ion. This approach proved problematic, as the highly charged uranium ion would polarize the water molecules, leaving the sulfate moiety almost naked. Therefore, a very large cluster consisting of 100 water molecules and one sulfate ion was optimized using the xTB method. Vibrational spectra were calculated and compared with experiment. The influence of the pH value was checked

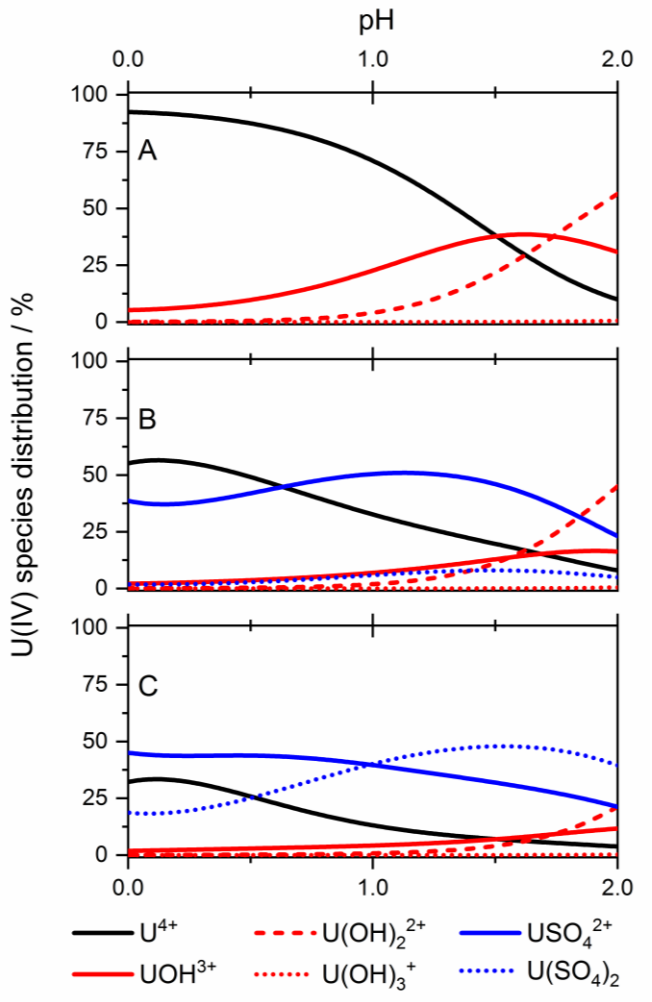

Figure 4: Speciation distribution calculated for 60 µM [U(IV)] at Eh = 0 mV and *I* = 0.15 M Na/HClO4 in pH range 0 to 2. A) Without sulfate; B) with 1 mM [SO_4^{2-}] using Data of NEA TDB[1]; C) with 1 mM [SO_4^{2-}] using log ß determined in this work.

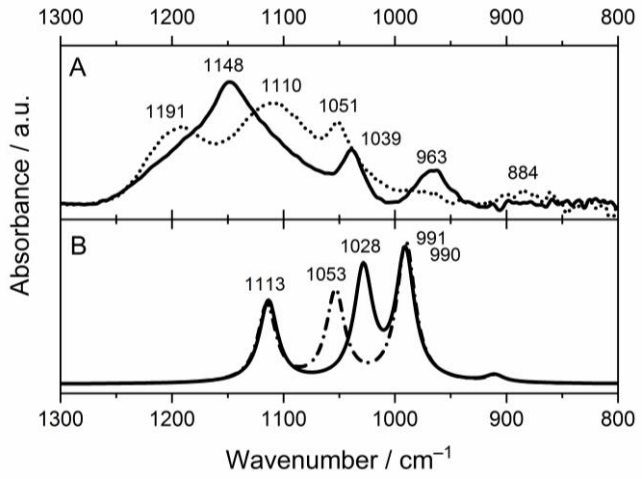

Figure 5: A) IR spectra of aqueous solution of sulfate (dotted trace) and the corresponding U(IV) species (solid trace). [Sulfate] = 1 mM; [U] = 2 mM; pH 1. B) Calculated IR spectra for the sulfate ion in an U(IV) sulfate complex with 100 water molecules. Original structure C1 is shown as solid trace. Dashed trace shows IR spectrum of one other optimized cluster C2 with the greatest deviation from C1.

by adding protons to the cluster. The IR spectra calculated with the xTB method can be found in the supporting information†. Full optimization with DFT for the sulfate containing water clusters was tried. The number of cycles needed was very large, due to the flexibility of the cluster, the optimization was stopped when the energy changes were very low. At this point the forces on some water molecules were still rather high and therefore the calculated IR spectra were not used for comparison with experiment. The uranium was then added to the optimized cluster and full DFT optimizations were performed. Because of the high charge of the uranium added, the cluster flexibility was diminished and optimization succeeded in a few hundred iterations. Three different starting geometries were considered: mono-, bi- and tridentate bonding of the sulfate ion. Upon optimization, no true minimum for the tridentate or bidentate motif could be found. Following the computed imaginary frequencies led to monodentate structures (Figure 6). These monodentate structures differ slightly in the position of the surrounding water molecules. As the clusters consist of 306 atoms, calculating the complete IR spectrum would have been very time consuming. To circumvent that problem, a frozen-density embedding like approach was taken. In the numerical calculations of the vibrational frequencies all atoms except the ones belonging to the sulfate ion were frozen. They were still present in the DFT calculations, but not moved for the calculation of vibrational frequencies.

Comparing Figure 5 A and B it can be seen, that the calculated and measured IR spectra agree quite well. It is interesting to investigate, how changes in the uranium sulfate bonding affect the IR spectrum. Further complexes with slightly different start U-$O_{sulfate}$ bonding distances were therefore prepared and optimized. In Figure 5 B, the IR spectrum of one other optimized cluster (C2) with the greatest deviation from the original structure (C1) is shown in dashed. There is a marked shift, but only for the middle of the three signals. The structural differences between the clusters can be seen in Figure SI 11 in the ESI†. The IR spectrum of C1 agrees slightly better with the experiment. The splitting between the three signals is 40 and 80 cm^{-1} for C1, for C2 this splitting is 60 and 60 cm^{-1}. Experimentally a splitting of 80 and 110 cm^{-1} is observed.

To understand the U-O bonds in the uranium sulfate system better, QTAIM calculations for the best structure (C1) were performed. From these calculations, the delocalization indices for the U-O and S-O bonds were extracted (see Table 4). The average U-O_{Water} bond length is 240 pm. The U-$O_{(SO4)}$ bond is 7 pm shorter. The DI for this bond is 1.2 and much higher than the average U-$O_{(H2O)}$ value of 0.8. This strong U-$O_{(SO4)}$ interaction weakens the neighboring S-O bond, the DI of which is 1.6. The other three S-O bonds show a significantly higher DI of 2.0. Although the fours S-O bonds are that different, the bond radii do not differ that much. The S-O distances seem to be dictated by the water cluster, the strong electron withdrawing effect of the U^{4+} leads to a reduced number of shared electrons but no significant change in distance.

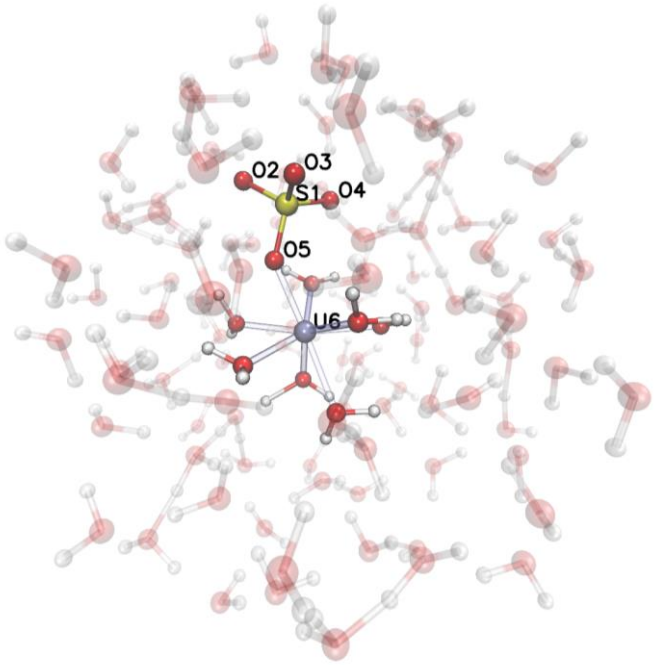

Figure 6: Best computational guess for the structure of the U(IV)SO_4 complex in aqueous solution. The sorrounding extra water molecules are rendered transparent in order to improve the clearness of the picture. Numbering of atoms is consecutive.

Table 4: Bond length (in pm) and delocalization indices (DI) for the important bonds in the USO_4^{2+} system. Numbering is equal to Figure 6.

Bond	Bond Length (in pm)	DI
U6-O5	233	1.2
S1-O2	154	2.0
S1-O3	151	2.0
S1-O4	152	2.0
S1-O5	154	1.6

Our computed U-S distance of 364 pm agrees well with the U-S distance of 367 pm for monodentate bonding as found in the EXAFS studies of Hennig et al.[19, 20] They have investigated different complexes with up to 5 sulfate ions per U(IV) and find both mono- and bidentate binding. Our speciation shows that for the concentrations used in this work USO_4^{2+} should be the dominant species and for this species clear monodentate binding should be the preferred mode.

Conclusions

U(IV) sulfate speciation as well as structural information in aqueous solution in the micro-/millimolar range were directly determined by a combination of UV/vis and ATR FT-IR spectroscopy, supported by quantum-chemistry. The high data quality even at these low uranium concentrations enabled the derivation of complex formation constants, single component spectra, extinction coefficients and species distribution for 1:1 and 1:2 complexes. Our thermodynamic results support former studies which used indirect methods or applied analogy

principles to other tetravalent actinides due to a lack of reliable direct data for U(IV). The gained reference spectra are an essential contribution for analysis of U(IV) in natural multicomponent systems. In this context, it is important to stress that sulfate exhibits a stronger impact on uranium speciation in reducing environments in comparison to oxidizing conditions (see Supplementary Material Figure SI 1 and Table SI 3[†]). The presented photometric measuring system was proven to be well applicable for speciation analysis at environmental relevant uranium concentrations.

Structural aspects of the sulfate species were derived from a combined approach of vibrational spectroscopy and quantum-chemical calculations evidencing a predominant monodentate coordination of the sulfate ligands. The slight change of the ligand field by monodentate coordination with sulfate results in only a small difference between UV/vis absorption spectra of U(IV) aquo ion and U(IV) sulfate species.

The approach of this work is transferrable to other ligands within the U(IV) system and to some extent to further tetravalent heavy metal ions. Therefore, this work potentially contributes to future studies of fundamental complexation reactions of metal ions in aqueous media. The results of this work shall not only promote the characterization of complex system as, e.g., encountered in nuclear waste management, but also identifying unknown uranium substances in environmental systems. Furthermore, conservatism and uncertainties applied so far in contaminant migration prognostics shall be reduced with the new thermodynamic data and species characterization, and consequently increase confidence in quantitative modeling. Hence, this study enables a more accurate prediction of U(IV) behavior in the environment.

Conflicts of interest

There are no conflicts to declare.

Acknowledgements

The authors kindly acknowledge funding by the German Ministry of Economic Affairs and Energy under the grants 02E11334B within the EDUKEM project: Development and application of experimental techniques to improve modelling of saline uranium containing solutions. The authors are grateful to S. Weiß for supporting electrochemical sample preparation. We thank S. Gurlit and B. Pfützner for ICP-MS measurements. We acknowledge as well K. Heim and P. Dullies for supporting ATR FT-IR measurements.

References

1. R. Guillaumont, T. Fanghänel, J. Fuger, I. Grenthe, V. Neck, D. A. Palmer and M. H. Rand, *Update on the chemical thermodynamics of uranium, neptunium, plutonium, americium and technetium*, Elsevier, Amsterdam, 2003.
2. M. Rand, J. Fuger, I. Grenthe, V. Neck and D. Rai, *Chemical Thermodynamics of Thorium*, Elsevier, Amsterdam, 2008.
3. K. A. Kraus and F. Nelson, *J Am Chem Soc*, 1950, **72**, 3901-3906.
4. E. L. Muhr-Ebert, F. Wagner and C. Walther, *Appl Geochem*, 2019, **100**, 213-222.
5. D. Rai, L. Rao, H. Weger, A. R. Felmy and G. R. Choppin, *Thermodynamic data for predicting concentrations of Th(IV), U(IV), Np(IV), and Pu(IV) in geologic environments*, Pacific Northwest National Laboratory, Richland, 1999.
6. G. Bernhard, G. Geipel, V. Brendler and H. Nitsche, *J Alloy Compd*, 1998, **271**, 201-205.
7. IAEA, *In situ leach uranium mining: an overview of operations*, Report No. NF-T-1.4, IAEA, Vienna, Austria, 2016.
8. J. Fuger, *Radiochim Acta*, 1992, **58-9**, 81-91.
9. P. L. Brown, E. Curti and B. Grambow, *Chemical Thermodynamics of Zirconium*, Elsevier, Amsterdam, 2005.
10. IAEA, *Manual of acid in situ leach uranium mining technology*, Report IAEA-TECDOC--1239, Vienna, Austria, 2001.
11. R. A. Day, R. N. Wilhite and F. D. Hamilton, *J Am Chem Soc*, 1955, **77**, 3180-3182.
12. R. H. Betts and R. M. Leigh, *Can J Res B*, 1950, **28**, 514-525.
13. J. C. Sullivan and J. C. Hindman, *J Am Chem Soc*, 1952, **74**, 6091-6096.
14. P. May, *Talanta*, 2010, **81**, 142-148.
15. A. R. Felmy and D. Rai, *J Solution Chem*, 1999, **28**, 533-553.
16. H. Majima, Y. Awakura, K. Sato and S. Hirono, *Metall Trans B*, 1987, **18**, 49-57.
17. H. Wanner, *Modelling Interaction of Deep Groundwaters with Bentonite and Radionuclide Speciation*, Report EIR-Report Nr. 589, Eidgenoessisches Institut für Reaktorforschung, Wuerenlingen, Switzerland, 1986.
18. R. D. Shannon, *Acta Crystallogr A*, 1976, **32**, 751-767.
19. C. Hennig, W. Kraus, F. Emmerling, A. Ikeda and A. C. Scheinost, *Inorg Chem*, 2008, **47**, 1634-1638.
20. C. Hennig, K. Schmeide, V. Brendler, H. Moll, S. Tsushima and A. C. Scheinost, *Inorg Chem*, 2007, **46**, 5882-5892.
21. K. Opel, S. Weiss, S. Hubener, H. Zanker and G. Bernhard, *Radiochim Acta*, 2007, **95**, 143-149.
22. R. Steudtner, S. Sachs, K. Schmeide, V. Brendler and G. Bernhard, *Radiochim Acta*, 2011, **99**, 687-692.
23. D. L. Parkhurst and C. A. J. Appelo, *Description of input and examples for PHREEQC version 3—A computer program for speciation, batch-reaction, one-dimensional transport, and inverse geochemical calculationss*, U.S. Geological Survey, U.S. Department of the Interior, Denver, Colorado, 2013.
24. C. M. Bethke, *Geochemical and Biogeochemical Reaction Modeling*, Cambridge University Press, Cambridge, 2 edn., 2010.
25. C. W. Davies, *Ion Association*, Butterworth, Washington, 1962.
26. L. Ciavatta, *Ann Chim*, 1980, **70**, 551-567.
27. K. S. Pitzer, *Can J Chem Eng*, 1991, 75-153.
28. R. J. Lemire, U. Berner, C. Musikas, D. A. Palmer, P. Taylor and O. Tochiyama, *Chemical Thermodynamics of Iron: Part I*, OECD Nuclear Energy Agency, Paris, 2013.

29. T. Thoenen, W. Hummel, U. Berner and E. Curti, *The PSI/Nagra Chemical Thermodynamic Database 12/07*, Report 14-04, Paul Scherrer Institut, Villigen, 2014.
30. H. C. Moog, F. Bok, C. M. Marquardt and V. Brendler, *Appl Geochem*, 2015, **55**, 72-84.
31. J. H. Yoe and A. L. Jones, *J Ind Eng Chem, Analytical edition*, 1944, **16**, 111-115.
32. P. Job, *Ann Chim France*, 1928, **9**, 113-203.
33. N. Jordan, M. Demnitz, H. Losch, S. Starke, V. Brendler and N. Huittinen, *Inorg Chem*, 2018, **57**, 7015-7024.
34. P. Gans, A. Sabatini and A. Vacca, *Talanta*, 1996, **43**, 1739-1753.
35. P. Gans, A. Sabatini and A. Vacca, *Ann Chim*, 1999, **89**, 45-49.
36. K. Gückel, S. Tsushima and H. Foerstendorf, *Dalton T*, 2013, **42**, 10172-10178.
37. S. Grimme, C. Bannwarth and P. Shushkov, *J Chem Theory Comput*, 2017, **13**, 1989-2009.
38. P. G. O'Shea and H. P. Freund, *Science*, 2001, **292**, 1853-1858.
39. J. P. Perdew, *Phys Rev B*, 1986, **33**, 8822-8824.
40. F. Weigend and R. Ahlrichs, *Phys Chem Chem Phys*, 2005, **7**, 3297-3305.
41. X. Y. Cao and M. Dolg, *J Mol Struc-Theochem*, 2004, **673**, 203-209.
42. S. Grimme, J. Antony, S. Ehrlich and H. Krieg, *J Chem Phys*, 2010, **132**.
43. A. Klamt and G. Schuurmann, *J Chem Soc Perk T 2*, 1993, 799-805.
44. T. A. Keith, AIMAll, 2019. (Version 19.02.13), TK Gristmill Software, Overland Park KS, USA, 2019 (aim.tkgristmill.com).
45. X. Fradera, M. A. Austen and R. F. W. Bader, *J Phys Chem A*, 1999, **103**, 304-314.
46. A. Kirishima, T. Kimura, R. Nagaishi and O. Tochiyama, *Radiochim Acta*, 2004, **92**, 705-710.
47. W. Cha, H. R. Cho, Y. S. Youn and E. C. Jung, Conference Abstract, 253rd National Meeting of the American Chemical Society, San Francisco, CA, 2017.
48. C. W. Davies and V. C. Patel, *J Chem Soc*, 1962, 880-&.
49. Y. X. Xia, L. F. Rao, D. Rai and A. R. Felmy, *Radiochim Acta*, 1999, **86**, 33-40.
50. K. Nakamoto, in *Handbook of Vibrational Spectroscopy*, ed. 1, Wiley, Chichester, 2002, pp. 1872-1892.